minerals

MDPI

Article

Effect of Dodecane and Oleic Acid on the Attachment between Oxidized Coal and Bubbles

Mengdi Xu [1], Yaowen Xing [1,2,*], Yijun Cao [3,4,*] and Xiahui Gui [4]

1 School of Chemical Engineering and Technology, China University of Mining and Technology, Xuzhou 221116, Jiangsu, China; cumtxmd@outlook.com
2 Max Planck Institute for Polymer Research, Ackermannweg 10, 55128 Mainz, Germany
3 Henan Province Industrial Technology Research Institute of Resources and Materials, Zhengzhou University, Zhengzhou 450001, China
4 Chinese National Engineering Research Center of Coal Preparation and Purification, China University of Mining and Technology, Xuzhou 221116, China; guixihaui1985@163.com
* Correspondence: cumtxyw@126.com (Y.X.); caoyj@cumt.edu.cn (Y.C.); Tel.: +86-0516-8359-1116 (Y.C.)

Received: 13 November 2017; Accepted: 12 January 2018; Published: 23 January 2018

Abstract: The objective of this study is to explain the different flotation responses observed in oxidized coal flotation when using a nonpolar flotation collector, dodecane, versus a polar flotation collector, oleic acid. Particularly, the effect of each flotation collector on bubble–coal particle attachment was investigated. Colloidal probe atomic force microscopy (AFM) was used to directly measure the force between a model coal surface and a model bubble in the presence of either dodecane or oleic acid. Pyrolytic graphite (PG) treated with oxygen plasma and a polymethylmethacrylate (PMMA) particle were selected to represent the model oxidized coal surface and model bubble. High speed visualization for bubble–oxidized coal attachment was used to monitor the attachment behavior between bubble and oxidized coal in presence of dodecane and oleic acid, respectively. It was found that the force between the oxidized PG and the PMMA particle in Milli-Q water was monotonically repulsive, illustrating that oxidized coal particles attach onto bubble surface with difficulty. The flotation recovery using a traditional hydrocarbon oil, dodecane, was always lower than when oleic acid was used at a low dosage (300–1100 g/t). The force measurements showed that an attractive hydrophobic force was introduced when a 0.01 mM oleic acid solution was used, while the force was still repulsive in presence of a 0.01 mM dodecane solution. The minimum contact time for successful attachment between oxidized coal surface and bubbles in the presence of 0.01 mM oleic acid is much shorter than that in 0.01 mM dodecane. However, a high flotation recovery of 85.81% was obtained when dodecane concentration was further increased to 1700 g/t. The significant jump into contact effect observed in the AFM force curves and the short induction time in the presence of 1 mM dodecane solution was responsible for this high flotation recovery.

Keywords: oxidized coal; flotation; dodecane; oleic acid; interaction force; AFM

1. Introduction

Re-utilization of oxidized coal slime waste is of practical importance for energy conservation and environment protection. However, upgrading the flotation process of oxidized coal using conventional nonpolar oily flotation collectors, such as diesel and kerosene, is difficult because of the abundance of oxygen-containing functional groups on the surface of the oxidized coal [1–3]. The presence of carboxylic acid, phenol, and carbonyl functional groups makes coal particles hydrophilic and prevents bubble–particle attachment during the flotation process.

It is well known that a polar oxygen-containing flotation collector can significantly increase the oxidized coal flotation recovery [4–6]. Jia et al. [5,6] used a series of oxygen-containing non-ionic

surfactants, tetrahydrofurfuryl esters (THF), as the collectors for low-rank/oxidized coal flotation. Hydrogen bonding between the oxidized coal surface and the polar collector was considered to be the mechanism of flotation intensification. Chang et al. [7] also found that a mixture of diesel and Triton X-100 was beneficial to the oxidized coal flotation process. The polar Triton X-100 collector concentration required to achieve a satisfactory recovery was found to be proportional to the degree of coal oxidation. Recently, Gui et al. [4] calculated the interfacial interaction energy between oxidized coal and two collectors, dodecane and α-furanacrylic acid, to identify the interaction mechanisms from a thermodynamic perspective. A new adsorption pattern was proposed, where water molecules in a hydration film around the oxidized coal act as a hydrogen-bonding bridge for α-furanacrylic acid adsorption onto the surface of the oxidized coal. Furthermore, the interaction forces between different types of collectors and oxidized coal were measured by Xing et al. [2] using colloidal atomic force microscopy (AFM). Solid-state paraffin and stearic acid were selected to represent a hydrocarbon oil and a fatty acid collector, respectively. A significant jump into contact effect between the oxidized coal particles and the stearic acid at a distance of 20 nm was observed, while there was a monotonically repulsive force between the oxidized coal and the paraffin, which correlated well with oxidized coal results using dodecane and oleic acid as collectors. However, a thorough investigation of the force and attachment behavior between the bubbles and the oxidized coal particles in the presence of collectors was neglected in the above studies. A more comprehensive understanding of how different types of collectors affect bubble–coal particle attachment is necessary.

AFM belongs to the family of scanning probe microscopy. It was first developed by Binnig et al. [8] in 1986, for imaging the surface topography at nanometer resolution [9]. A sharp probe mounted near the end of a cantilever is raster scanned along the sample surface. A laser beam was used to monitor the deflection of the cantilever via a position sensitive diode (PSD) detector. Cantilever deflection is proportional to the force acting on the tip. Usually, a feedback loop is used to keep the force between tip and sample constant by moving the sample up and down during scanning. In that case, the height of the sample is plotted versus the lateral position to obtain a three-dimensional topographic image both in air or liquid condition [10–12]. Soon after, AFM was used as a force sensor to measure forces—including surface forces, adhesion force, and hydrodynamic force—between different surfaces or molecules of interest, especially with the aid of the so called "colloidal probe technique" [13,14]. The force is obtained by multiplying the spring constant of the cantilever and the deflection. In the colloid probe technique, a micrometer-size particle with well-defined geometry is attached to the end of the cantilever in order to replace the sharp tip. Usually, the particle is spherical to facilitate the quantitative analysis. Thus, the interaction geometry between the probe and surface is greatly simplified. Currently, AFM has matured to an indispensable surface analytical tool to characterize nanomaterial in colloid and interface science. In the last two decades, AFM has also been widely used by flotation scientists to image mineral morphology and measure the force between single particles, greatly assisting the fundamental understanding of large-scale flotation. Although, from the flotation engineering point of view, such single-particle level information is difficult to predict flotation recovery directly since a large number of particles are always involved in flotation practice, it can still provide useful input parameters for computational fluid dynamics simulation to design a high efficiency flotation process. In recent years, progress has been made on the studies of bubble–particle attachment using AFM [15–19]. However, the direct force measurement between an air bubble and a solid particle is always accompanied by the deformation of the gas–liquid interface by both the hydrodynamic and surface forces [20]. This poses a challenge in determining the absolute separation and the surface force between the bubbles and the particles in water. Datta et al. [21] proposed that the air bubble could be substituted with a hydrophobic polystyrene (PS) sphere for the AFM force measurements. Although the adsorption behavior of a surfactant on an air–water interface is different from the behavior on a PS–water interface, such complementary data would provide a more detailed description of the effect of surfactants on bubble–coal particle interaction.

The objective of this study is to explain the different flotation responses of a nonpolar collector, dodecane, and a polar collector, oleic acid, in oxidized coal flotation process, with emphasis on how they affect the bubble–coal particle attachment. Colloidal probe AFM was used to directly measure the force between a model coal surface and a model bubble in the presence of either dodecane or oleic acid. Pyrolytic graphite (PG) after oxygen plasma treatment and a polymethylmethacrylate (PMMA) particle were selected to represent the oxidized coal and bubbles, respectively. High speed visualization for bubble–oxidized coal attachment was used to monitor the attachment behavior between bubble and oxidized coal in presence of dodecane and oleic acid, respectively.

2. Materials and Methods

2.1. Materials

Fresh fine-coal samples with 18.47% ash content were collected from the Xuehu Coal Preparation Plant coal storage yard in Yongcheng City, Henan Province, China. The oxidized coal samples were prepared by the hydrogen peroxide oxidation method. Fresh coal samples were immersed in 30% hydrogen peroxide solutions for 6 h in an agitator at 400 rpm [2]. Scanning electron microscopy (SEM) and X-ray photoelectron spectroscopy (XPS) were used to examine the surface properties of the oxidized coal. The SEM images and Cls peaks of the oxidized coal are shown in Figures 1 and 2, respectively. For comparison, an SEM image of fresh coal is also shown in Figure 1. The oxidized coal showed a more rugged morphology and contained more grey flakes than those of a fresh coal sample. The oxygen containing groups, C–O, C=O, and O=C–O, accounted for 27.17% of the surface area of the oxidized coal. The abundance of these oxygen-containing groups make oxidized coal hydrophilic.

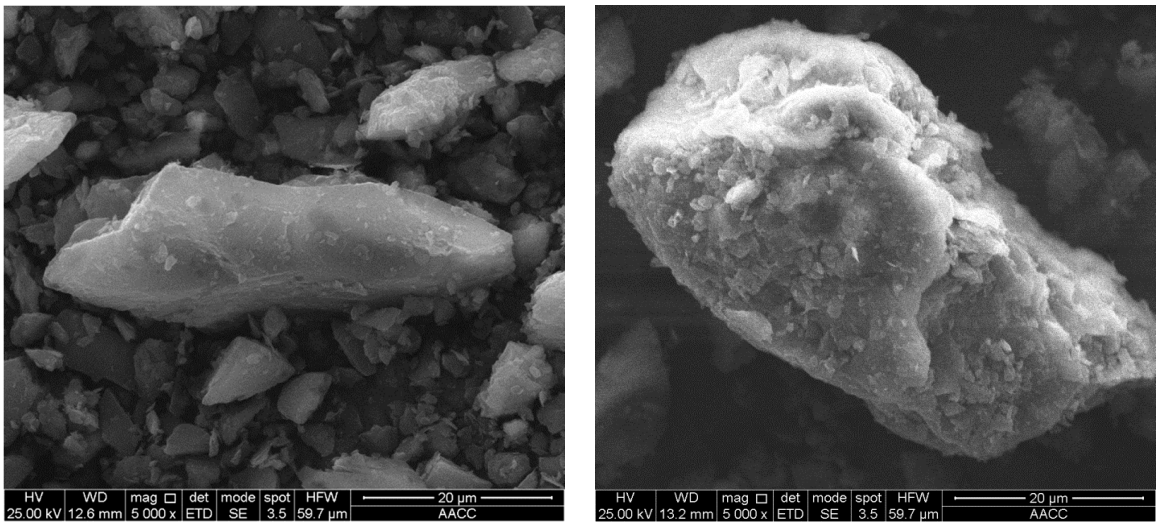

(**a**) (**b**)

Figure 1. SEM images of fresh (**a**) and oxidized coal (**b**).

Two flotation collectors, dodecane and oleic acid, were purchased from Sinopharm Chemical Reagent Co., Ltd, (Shanghai, China). For the AFM force measurement, a fresh PG planchet (Electron Microscopy Sciences) was oxidized via oxygen plasma treatment for 10 min. The PMMA microspheres with 6.44 µm diameter used in this study were purchased from Bangs Laboratories Inc, (Fisher, IN, USA). An HA-C/tipless cantilever (NT-MDT, Spectrum Instruments, Moscow, Russia) with a nominal spring-constant of 0.65 N/m was chosen to prepare the PMMA colloidal probe.

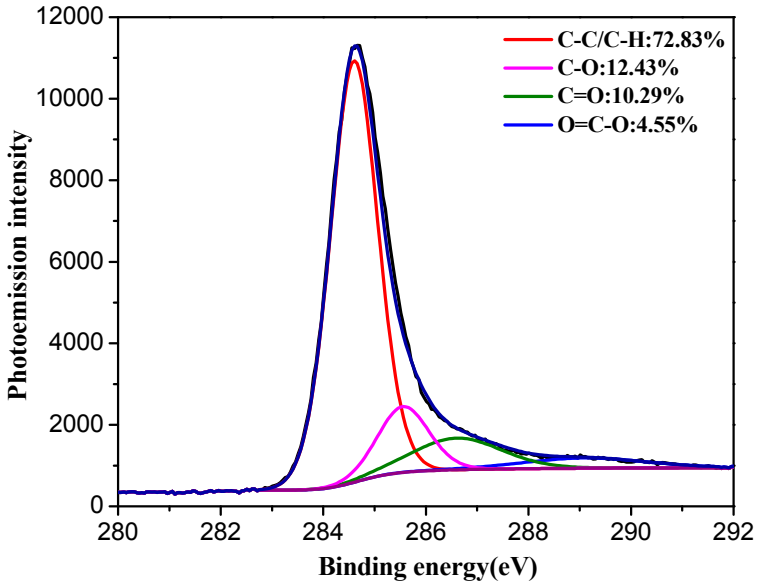

Figure 2. Cls peak of oxidized coal.

2.2. Methods

2.2.1. Flotation Experiments

Oxidized coal flotation experiments were carried out in an XFDIII 1 dm^3 laboratory flotation machine. A range of flotation collector concentrations were used: 300, 500, 700, 900, 1100, 1500, and 1700 g/t for dodecane; and 300, 500, 700, 900, and 1100 g/t for oleic acid. The concentration of the frothing agent, octanol, and the impeller rotation were kept constant at 100 g/t and 1800 rpm, respectively. It should be noted that the use of octanol as a frother produces a stable foam, but it may cause hydrophobization of the raw material or the gangue. The solid content and the air flow rate were kept at constant values of 80 g/dm^3 and 0.15 m^3/h, respectively. The pulp was pre-wetted for 2 min. After the pre-wetting process, the flotation collector and the frothing agent were added to the pulp stepwise. The flotation collector and the frothing agent conditioning processes were maintained for 2 min and 0.5 min, respectively. At the end of conditioning period, bubbles began forming froth on the upper pulp surface. The flotation process was maintained for another 3 min. The flotation process formed concentrates and tailings; both were collected, filtered, dried, and then sent for ash analysis.

2.2.2. AFM Force Measurements

Force measurements between the oxidized PG surface and PMMA colloidal probe in the presence of dodecane and oleic acid were carried out using a NanoWizard™ III AFM (JPK Instrument, Berlin, Germany). Two concentrations of the collector, 0.01 mM and 1 mM, were selected. To prepare the PMMA colloidal probe, a hydraulic micromanipulator (Narishige MMO-203, Tokyo, Japan) and an optical microscope (Zeiss Axiotech, Oberkochen, Germany) were used. The cantilever was first dipped into a small amount of epoxy resin and then moved onto a PMMA microsphere. By slightly lowering the cantilever, the PMMA sphere could be attached at the end of cantilever, as shown in Figure 3a. Before the force experiments, the sensitivity and spring constant of the colloidal probe were obtained using JPK's software. Interaction forces were obtained by recording the cantilever deflection via an optical sensitive lever technique, as shown in Figure 3b. During the force measurements, the approach speed was fixed at 1 μm/s. Three force curves were collected at one position, and the general trends are presented in this paper. All experiments were conducted at room temperature (20 °C).

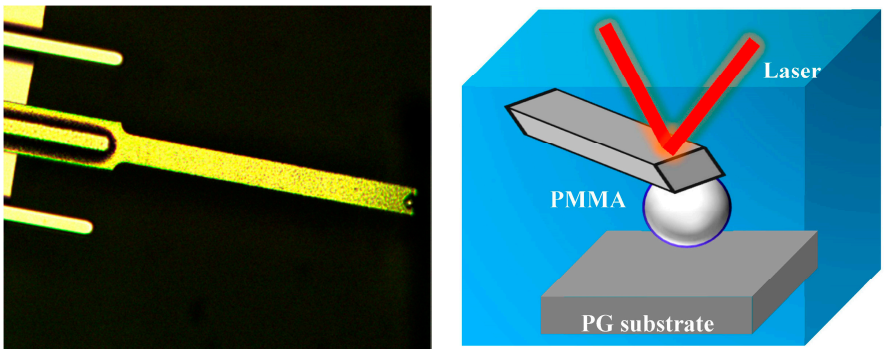

Figure 3. PMMA colloid probe (**a**) and the schematic of force measurement (**b**). The width of cantilever is 34 μm.

2.2.3. High Speed Visualization for Bubble–Oxidized Coal Attachment

A home-made system, high speed visualization for bubble–oxidized coal attachment (as shown on Figure 4), was used to monitor the attachment behavior between bubble and oxidized coal in presence of dodecane and oleic acid, respectively. Actually, the system is, to some extent, similar to a traditional induction timer [2], which consists of a light source, a high speed camera, a displacement stage, a micro-syringe, and a picomotor piezo linear actuator. An air bubble is created using the micro-syringe at the tip of a capillary, which can be moved up and down by the picomotor actuator (New Focus^{TM}, Irvine, CA, USA) with a 30 nm positioning resolution. The bubble remains in contact with sample substrate for a given time till the bubble is retracted. The high speed camera is used to record whether successful attachment can occur or not. The minimum time for successful attachment is defined as the induction time. It should be noted that, due to the limitation of time control accuracy of our system, the time value we obtained is not the real induction time. Nevertheless, some complementary information on bubble–oxidized coal attachment can be obtained. During the experiment, a flat oxidized coal substrate was used and the concentrations of the collector were same with those used in AFM experiments. The bubble diameter, maximum displacement of the capillary tube, initial distance gap, and approach velocity were all kept constant in all tests.

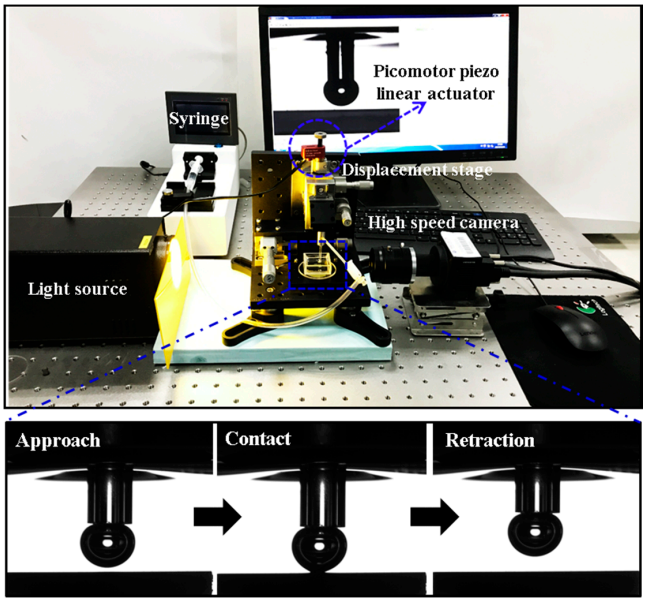

Figure 4. High speed visualization system for bubble–oxidized coal attachment.

3. Results and Discussion

3.1. Oxidized Coal Flotation Using Dodecane and Oleic Acid

The oxidized coal flotation results using dodecane as a flotation collector are shown in Figure 4. For comparison, a fresh coal flotation experiment using 300 g/t of dodecane was also conducted. The fresh coal sample resulted in 91.98% combustible recovery and 50.24% ash recovery. When the coal was oxidized, the combustible recovery significantly decreased to 42.28% under the same dodecane concentration, as shown in Figure 5. This illustrated that the oxidized coal became difficult to float after oxidation due to the introduction of oxygen-containing groups. As the concentration of dodecane was increased, both the combustible recovery and the ash recovery increased. It should be noted that when the dodecane concentration increased from 1500 g/t to 1700 g/t, the combustible recovery abruptly increased from 65.18% to 85.81%. This sudden jump in combustible recovery indicates that obtaining a satisfactory oxidized coal flotation recovery is still possible when using dodecane, albeit at a high concentration.

The oxidized coal flotation results using oleic acid as a flotation collector are shown in Figure 6. The flotation recovery with oleic acid was always higher than when using dodecane at low concentrations (300–1100 g/t). Hydrogen bonding between C–O and C=O groups on the coal's surface and the carboxyl group in oleic acid was responsible for this flotation response. For example, a combustible recovery of 62.33% was obtained when 300 g/t of oleic acid was used. A combustible recovery of 77.76% with an ash recovery of 41.78% was obtained when 700 g/t of oleic acid was used. When the flotation collector concentration was further increased, the combustible recovery did not change significantly, while the ash recovery increased dramatically. This is probably due to the foaming function of oleic acid, enhancing water entrainment and thus deteriorating flotation selectivity. On the other hand, oleic acid also can increase the float of silica and other gangue minerals, resulting in the increase in the ash content of the clean coal products. When oleic acid dosage increased to 700–900 g/t, it could be absorbed on the surface of bubbles, decreasing the hydrophobicity of bubble surface, thus preventing the attachment of coal particles to bubble surface. Therefore, combustible recovery remains constant or even declines.

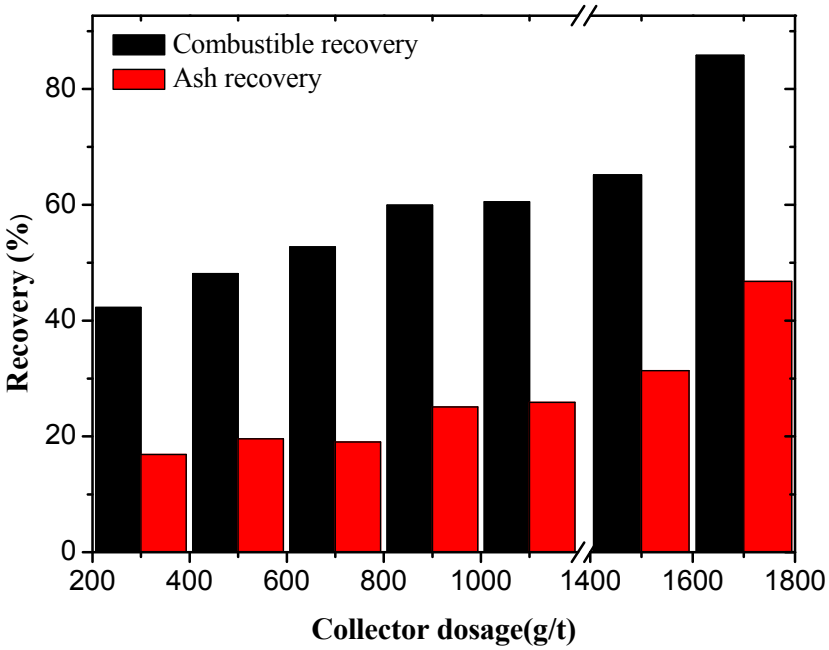

Figure 5. Oxidized coal flotation results using dodecane.

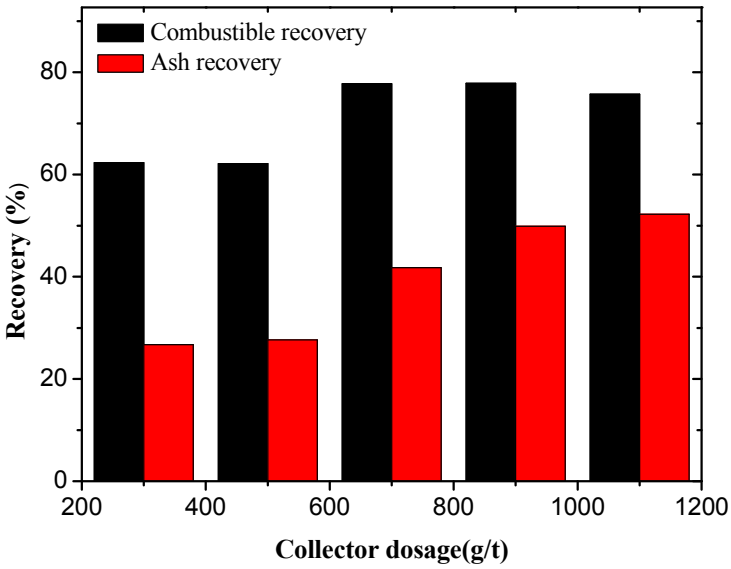

Figure 6. Oxidized coal flotation results using oleic acid.

3.2. Forces between Oxidized PG Surface and PMMA Colloidal Probe in the Presence of Dodecane and Oleic Acid

To explain the different flotation responses of the two flotation collectors used in oxidized coal flotation (Section 3.1), dodecane and oleic acid, the force between a model coal surface (oxidized PG) and a model bubble (PMMA) in the presence of either dodecane or oleic acid was measured. For comparison, we first measured the force between the PMMA colloid probe and a fresh sample of highly oriented PG (HOPG)/oxidized PG in Milli-Q water, as shown in Figure 7. It was found that a significant jump into contact effect at a distance of 25 nm was observed when the PMMA particle approached the fresh HOPG surface. At a distance of ~25 nm, the van der Waals force between the PMMA bubble and the hydrophobic HOPG is not yet significant, while the repulsive electrostatic double layer force should dominate the overall force behavior. Therefore, an attractive hydrophobic force is the driving force for this jump into attachment, although its origin is still under debate [22–25]. This phenomenon is consistent with hydrophobic particle–bubble interactions, where both the van der Waals force and the double layer force are repulsive, and the interaction is mainly because of the hydrophobic force. This observation also indicates that a hydrophobic PMMA particle is an appropriate model for an air bubble in AFM force measurements. In contrast, a monotonically repulsive force between the PMMA and the oxidized PG was observed in the AFM force curve due to the disappearance of the hydrophobic force. After oxygen plasma treatment, the water contact angle of PG surface was below 10°. Water molecules hydrogen bond with the oxidized PG, which decreases the hydrophobic effect. In this case, there is no attractive force to overcome the repulsive dispersion and double layer forces. This is consistent with the oxidized coal flotation results in which the flotation combustible recovery decreased from 91.98% to 42.38% after oxidation with 300 g/t of dodecane.

The force between the PMMA colloid probe and the oxidized PG in the presence of dodecane is shown in Figure 8. In the presence of a 0.01 mM dodecane solution, the force was repulsive over the entire distance range. However, an obvious jump into contact was observed when the dodecane concentration was increased to 1 mM. This observation indicated that small amounts of dodecane are insufficient to make the oxidized PG surface hydrophobic and that repulsive forces still dominate the PMMA–oxidized PG interaction. In contrast, attractive hydrophobic forces would re-dominate the force once a large amount of dodecane was used. This is consistent with the oxidized coal flotation results when dodecane is used as the collector. Thus, a satisfactory flotation recovery from oxidized coal was obtained when a high concentration of dodecane was used.

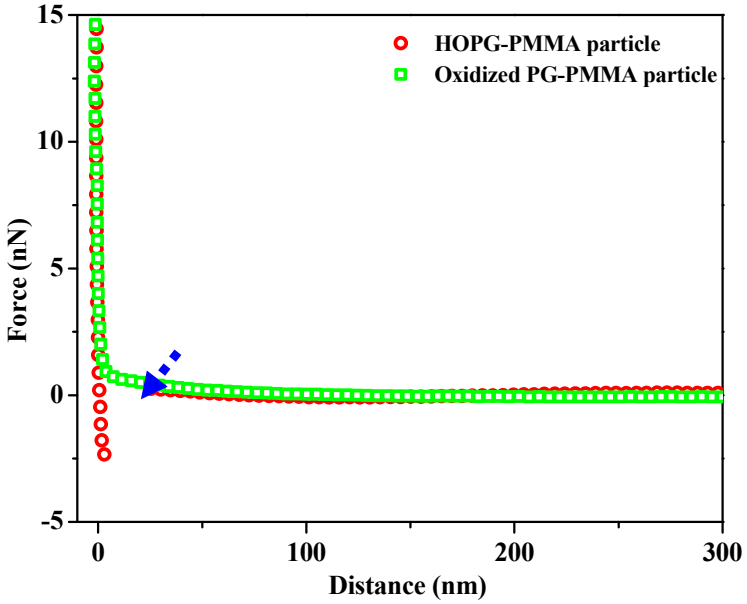

Figure 7. Force between PMMA colloid probe and HOPG/oxidized PG. Only approach force curves were shown.

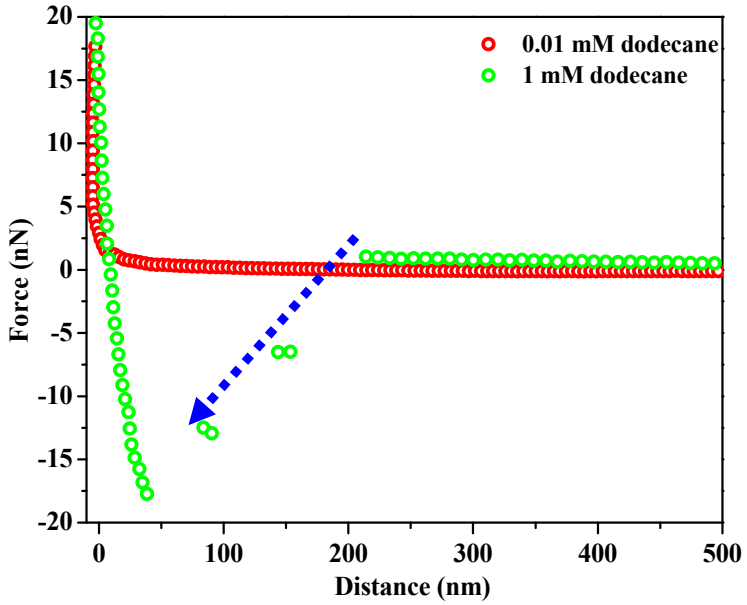

Figure 8. Force between PMMA colloid probe and oxidized PG in presence of dodecane. Only approach force curves were shown.

The force between the PMMA colloid probe and the oxidized PG in the presence of oleic acid is shown in Figure 9. Interestingly, a jump into attachment was observed in the presence of a 0.01 mM oleic acid solution. As the oleic acid concentration increased, both the jump into distance and the adhesion force increased. These observations illustrate that a small amount of oleic acid is enough to make the oxidized PG surface hydrophobic; thus, a hydrophobic force was introduced. This result explains why the flotation recovery was always higher when using oleic acid compared to that achieved when dodecane used at low concentrations (300–1100 g/t).

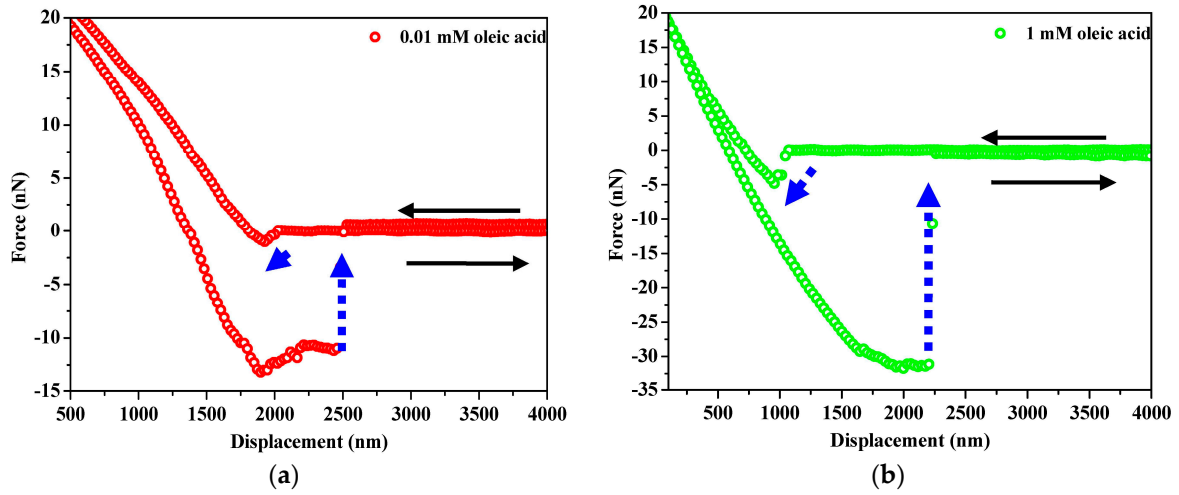

Figure 9. Force between PMMA colloid probe and oxidized PG in presence of oleic acid: (**a**) 0.01 mM oleic acid; (**b**) 1 mM oleic acid.

3.3. High Speed Visualization for Bubble–Oxidized Coal Attachment in the Presence of Dodecane and Oleic Acid

Snapshots of bubble–oxidized coal attachment observed at the minimum contact time in presence of different concentrations of docecane and oleic acid are shown in Figure 10. For docecane, when the concentration was 0.01 mM, the minimum contact time for successful bubble–particle attachment observed in our experimental system is 8 s. As the concentration increase to 1 mM, the contact time value dramatically decreased to 0.9 s, which is consistent with the results of flotation and AFM tests. The attractive hydrophobic force is responsible for the decrease in the minimum contact time for successful attachment. In contrast, for oleic acid, the minimum contact time for successful attachment is only 0.01 s both in 0.01 mM and 1 mM concentrations. It indicates that oleic acid is a kind of highly effective collector for oxidized coal flotation due to the short induction time.

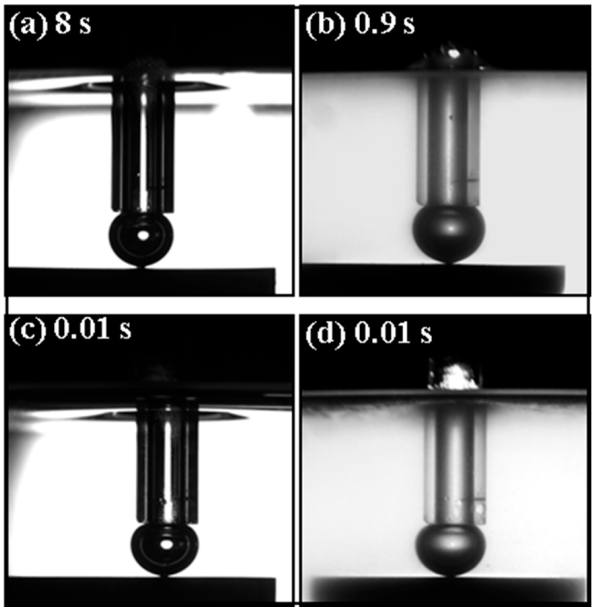

Figure 10. Snapshots of bubble–oxidized coal attachment observed at the minimum contact time in presence of different concentrations of docecane and oleic acid: (**a**) 0.01 mM dodecane; (**b**) 1 mM dodecane; (**c**) 0.01 mM oleic acid; (**d**) 1 mM oleic acid.

4. Conclusions

We have investigated the different flotation responses of both a nonpolar flotation collector, dodecane, and a polar flotation collector, oleic acid, on oxidized coal flotation. Particularly, we looked at how the presence of each flotation collector affects bubble–coal particle attachment by using a colloidal probe AFM technique to directly measure the force between a model coal surface (PG) and a model bubble (PMMA). The results showed that the force between the oxidized PG and the PMMA particle in Milli-Q water was monotonically repulsive, illustrating that the oxidized coal particles were difficult to float. The flotation recovery using the traditional hydrocarbon oil, dodecane, was always lower than when oleic acid was used at a low concentration (300–1100 g/t). The force measurements showed that an attractive hydrophobic force was introduced when a 0.01 mM oleic acid solution was used, while the force was still repulsive in the presence of a 0.01 mM dodecane solution. The minimum contact time for successful attachment between oxidized coal surface and bubble in the presence of 0.01 mM oleic acid is much shorter than that in 0.01 mM dodecane. However, a high flotation recovery of 85.81% was obtained when dodecane concentration was further increased to 1700 g/t. The significant jump into contact effect observed in the AFM force curves and the short induction time in the presence of 1 mM dodecane solution was responsible for this high flotation recovery.

Acknowledgments: This research was supported by the National Nature Science Foundation of China (Grant No. 51774286, 51574240), and Guizhou "125 plan" key project of science and technology project (No. Qian jiao he zhong da zhuang xiang zi [2013] 026) for which the authors express their appreciation.

Author Contributions: Y.X. conceived and designed the experiments; Y.X. and M.X. performed the experiments; X.G. and Y.C. analyzed the data; M.X. and Y.X. wrote the paper.

Conflicts of Interest: The authors declare no conflict of interest.

References

1. Xing, Y.; Gui, X.; Cao, Y.; Wang, Y.; Xu, M.; Wang, D.; Li, C. Effect of compound collector and blending frother on froth stability and flotation performance of oxidized coal. *Powder Technol.* **2017**, *305*, 166–173. [CrossRef]
2. Xing, Y.; Li, C.; Gui, X.; Cao, Y. Interaction forces between paraffin/stearic acid and fresh/oxidized coal particles measured by atomic force microscopy. *Energy Fuels* **2017**, *31*, 3305–3312. [CrossRef]
3. Xia, W.; Yang, J.; Liang, C. A short review of improvement in flotation of low rank/oxidized coals by pretreatments. *Powder Technol.* **2013**, *237*, 1–8. [CrossRef]
4. Gui, X.; Xing, Y.; Wang, T.; Cao, Y.; Miao, Z.; Xu, M. Intensification mechanism of oxidized coal flotation by using oxygen-containing collector α-furanacrylic acid. *Powder Technol.* **2017**, *305*, 109–116. [CrossRef]
5. Jia, R.; Harris, G.; Fuerstenau, D. An improved class of universal collectors for the flotation of oxidized and/or low-rank coal. *Int. J. Miner. Process.* **2000**, *58*, 99–118. [CrossRef]
6. Jia, R.; Harris, G.; Fuerstenau, D. Chemical reagents for enhanced coal flotation. *Int. J. Coal Prep. Util.* **2002**, *22*, 123–149. [CrossRef]
7. Chang, Z.; Chen, X.; Peng, Y. Understanding and improving the flotation of coals with different degrees of surface oxidation. *Powder Technol.* **2017**, *321*, 190–196. [CrossRef]
8. Binnig, G.; Quate, C.F.; Gerber, C. Atomic Force Microscope. *Phys. Rev. Lett.* **1986**, *56*, 930–933. [CrossRef] [PubMed]
9. Drake, B.; Prater, C.B.; Weisenhorn, A.L.; Gould, S.A.; Albrecht, T.R.; Quate, C.F.; Cannell, D.S.; Hansma, H.G.; Hansma, P.K. Imaging Crystals, Polymers, and Processes in Water with the Atomic Force Microscope. *Science* **1989**, *243*, 1586–1589. [CrossRef] [PubMed]
10. Butt, H.J.; Berger, R.; Bonaccurso, E.; Chen, Y.; Wang, J. Impact of atomic force microscopy on interface and colloid science. *Adv. Colloid Interface Sci.* **2007**, *133*, 91–104. [CrossRef] [PubMed]
11. Rugar, D.; Hansma, P. Atomic force microscopy. *Phys. Today* **1990**, *43*, 23–30. [CrossRef]
12. Meyer, E. Atomic force microscopy. *Prog. Surf. Sci.* **1992**, *41*, 3–49. [CrossRef]
13. Ducker, W.A.; Senden, T.J.; Pashley, R.M. Direct measurement of colloidal forces using an atomic force microscope. *Nature* **1991**, *353*, 239–241. [CrossRef]

14. Butt, H.-J. Measuring electrostatic, van der Waals, and hydration forces in electrolyte solutions with an atomic force microscope. *Biophys. J.* **1991**, *60*, 1438–1444. [CrossRef]
15. Butt, H.; Cappella, B.; Kappl, M. Force measurements with the atomic force microscope: Technique, interpretation and applications. *Surf. Sci. Rep.* **2005**, *59*, 1–152. [CrossRef]
16. Gillies, G.; Kappl, M.; Butt, H.J. Direct measurements of particle-bubble interactions. *Adv. Colloid Interface Sci.* **2005**, *114*, 165–172. [CrossRef] [PubMed]
17. Ducker, W.; Xu, Z.; Israelachvili, J.N. Measurements of hydrophobic and DLVO forces in bubble-surface interactions in aqueous solutions. *Langmuir* **1994**, *10*, 3279–3289. [CrossRef]
18. Butt, H.J. A technique for measuring the force between a colloidal particle in water and a bubble. *J. Colloid Interface Sci.* **1994**, *166*, 109–117. [CrossRef]
19. Assemi, S.; Nguyen, A.; Miller, J. Direct measurement of particle-bubble interaction forces using atomic force microscopy. *Int. J. Miner. Process.* **2008**, *89*, 65–70. [CrossRef]
20. Xing, Y.; Gui, X.; Pan, L.; Pinchasik, B.; Cao, Y.; Liu, J.; Kappl, M.; Butt, H. Recent experimental advances for understanding bubble-particle attachment in flotation. *Adv. Colloid Interface Sci.* **2017**, *246*, 105–142. [CrossRef] [PubMed]
21. Datta, A.; Nalaskowski, J.; Paruchuri, V.; Miller, J. Interaction forces between a coal surface and a polystyrene sphere in the presence of cationic and anionic surfactants as measured using atomic force microscopy. *Coal Perp.* **2000**, *21*, 337–353. [CrossRef]
22. Claesson, P.M.; Ederth, T.; Bergeron, V.; Rutland, M.W. Techniques for measuring surface forces. *Adv. Colloid Interface Sci.* **1996**, *67*, 119–183. [CrossRef]
23. Meyer, E.E.; Rosenberg, K.J.; Israelachvili, J. Recent progress in understanding hydrophobic interactions. *Proc. Natl. Acad. Sci. USA* **2006**, *103*, 15739–15746. [CrossRef] [PubMed]
24. Xing, Y.; Gui, X.; Cao, Y. The hydrophobic force for bubble-particle attachment in flotation-a brief review. *Phys. Chem. Chem. Phys.* **2017**, *19*, 24421–24435. [CrossRef] [PubMed]
25. Ralston, J.; Fornasiero, D.; Mishchuk, N. The hydrophobic force in flotation-a critique. *Colloids Surf. A* **2001**, *192*, 39–51. [CrossRef]